[Regular Paper]

Oxidative Dehydrogenation of Propane over Vanadate Catalysts Supported on Calcium and Strontium Hydroxyapatites

Shigeru SUGIYAMA[†1),†2),†3)]*, Takeshi OSAKA[†3)], Yohei UENO[†3)], and Ken-Ichiro SOTOWA[†1),†2),†3)]

[†1)] Dept. of Advanced Materials, Institute of Technology and Science, The University of Tokushima, Minamijosanjima, Tokushima 770-8506, JAPAN
[†2)] Dept. of Geosphere Environment and Energy, Center for Frontier Research of Engineering, The University of Tokushima, Minamijosanjima, Tokushima 770-8506, JAPAN
[†3)] Dept. of Chemical Science and Technology, The University of Tokushima, Minamijosanjima, Tokushima 770-8506, JAPAN

(Received June 6, 2007)

The oxidative dehydrogenation of propane to propylene was investigated over vanadate catalysts supported on calcium and strontium hydroxyapatites (VO_x/CaHAp and VO_x/SrHAp, respectively). Catalytic activities were improved by both CaHAp and SrHAp supports, but the improvement was greater for VO_x/SrHAp than for VO_x/CaHAp. The maximum yield of propylene observed for 5% VO_x/SrHAp was comparable to that of $Mg_2V_2O_7$, which is one of the most active catalysts for the oxidative dehydrogenation of propane. The combination of active sites for loading (VO_x) and the OH groups of the support (CaHAp and SrHAp) resulted in the enhanced catalytic activity. Furthermore, the redox nature of the loading directly contributed to the enhancement of VO_x/SrHAp activity. The effect of catalyst weight (5% VO_x/SrHAp) relative to the feedstock flow rate on selectivities to propylene and CO_x suggested that oxidative dehydrogenation proceeded through a consecutive mechanism in which propylene was formed from the oxidative dehydrogenation of propane, followed by deep oxidation from propylene to CO_x, rather than the direct oxidation of propane.

Keywords
Oxidative dehydrogenation, Propane, Hydroxyapatite support, Vanadate catalyst, Redox

1. Introduction

Our previous study suggested that the combination of OH groups in hydroxyapatite ($M_{10}(PO_4)_6(OH)_2$, M = divalent cation) and vanadate (VO_x) would form an active catalyst for the oxidative dehydrogenation of propane. In order to combine OH groups and vanadates, PO_4^{3-} in calcium hydroxyapatite ($Ca_{10}(PO_4)_6(OH)_2$; CaHAp) was partly substituted with VO_4^{3-} at the atomic ratio of V/P = 0.10 to form $Ca_{10}(PO_4)_{5.45}(VO_4)_{0.55}(OH)_2$ (VO_4–CaHAp), which had catalytic activity (16.5% of the conversion of propane and 54.2% of the selectivity to propylene)[1),2)], comparable to that of magnesium pyro-vanadate ($Mg_2V_2O_7$), which is one of most active catalysts for the oxidative dehydrogenation of propane[3)~6)]. Only CaHAp demonstrated rather low activity. However, the substitution of vanadate resulted in unfavorable modification of the hydroxyapatite structure. For example, increasing the vanadate contents in VO_4–CaHAp caused the hydroxyapatite structure to become an amorphous phase[1),2)]. Preliminary experiments showed that substitution of a small amount of PO_4^{3-} with VO_4^{3-} in strontium hydroxyapatite ($Sr_{10}(PO_4)_6(OH)_2$; SrHAp), with an atomic ratio of V/P = 0.025, (the latter had greater activity than that of CaHAp under the same reaction conditions as employed for CaHAp and VO_4–CaHAp systems)[1),2)], resulted in unfavorable conversion of $Sr_{10}(PO_4)_6(OH)_2$ to $Sr_2P_2O_7$. Since SrHAp showed higher activity for the oxidative dehydrogenation of propane to propylene than CaHAp, another process for the combination of OH groups in hydroxyapatite and vanadate should be developed. In this respect, supported catalysts, rather than substituted catalysts, seem to be more favorable for the combination of these two active species.

In the present study, vanadate was supported on both CaHAp and SrHAp for use as catalysts for the oxidative dehydrogenation of propane. Since the combination of vanadate and SrHAp provided an active catalyst comparable to $Mg_2V_2O_7$, the redox nature of the supported catalyst (VO_x/SrHAp) and its reaction mechanism for the oxidative dehydrogenation of propane was also investigated.

* To whom correspondence should be addressed.
* E-mail: sugiyama@chem.tokushima-u.ac.jp

2. Experimental

2. 1. Preparation of Vanadate-supported Calcium and Strontium Hydroxyapatites

All chemicals were of high purity and were used as supplied. Calcium and strontium hydroxyapatites (CaHAp and SrHAp, respectively) were prepared from $Ca(NO_3)_2 \cdot 4H_2O$ (Wako Pure Chemicals, Osaka) and $Sr(NO_3)_2$ (Wako) together with $(NH_4)_2HPO_4$ (Wako) according to the procedures reported by Hayek and Newsely[7] and Matsumura *et al.*[8]. The resulting solids were dried in air at 373 K overnight and then sieved to the size fraction of 0.85-1.70 mm, followed by calcination at 773 K for 3 h. Vanadate catalysts supported over CaHAp and SrHAp (VO_x/CaHAp and VO_x/SrHAp, respectively) were prepared from the supports by impregnation with an aqueous solution of NH_4VO_3 (Wako), followed by calcination at 773 K for 3 h. The loading is expressed as the weight percentage: 100V/(V + CaHAp) or 100V/(V + SrHAp).

2. 2. Apparatus, Procedure and Analysis

The catalytic experiments were performed in a fixed-bed continuous-flow reactor operated at atmospheric pressure. The reactor consisted of a quartz tube, 9 mm i.d. and 35 mm length, attached at each end to a 4 mm i.d. quartz tube for a total length of 25 cm. The catalyst charge was held in place in the enlarged portion of the reactor by two quartz wool plugs. In all experiments, the catalysts (0.5 g) were heated to the reaction temperature (723 K) while maintaining a continuous flow of helium and were held at this temperature under a 25 ml/min flow of oxygen for 1 h. The oxygen was then completely replaced by helium, and the reaction gas was introduced into the reactor. The reaction conditions are as follows unless otherwise stated: $P(C_3H_8)$ = 14.4 kPa, $P(O_2)$ = 4.1 or 0 kPa and F = 30 ml/min. No homogeneous reaction was observed under these conditions.

The reaction was monitored with an on-stream Shimadzu GC-8APT gas chromatograph equipped with a thermal conductivity detector and integrator (Shimadzu C-R6A). Two columns, one Porapak Q (6 m × 3 mm) and the other Molecular Sieve 5A (0.2 m × 3 mm), were employed in the analysis. The conversion of propane was calculated from the products and from the propane introduced into the feed. The selectivities were calculated from the conversion of propane to each product on a carbon basis. The yield of propylene was estimated from the conversion of propane multiplied by 1/100 of the selectivity to propylene. The carbon mass balances were 100 ± 5%. The reaction rate per unit of surface area was estimated as the rate per unit of catalyst weight ($r = FC_0X/W$, in which F, C_0, X and W are flow rate, initial concentration of C_3H_8, conversion of C_3H_8 and catalyst weight, respectively) divided by the catalyst surface area[9]. Continuous analyses of the reaction used the effluent gas from the reactor was introduced into a quadrupole mass spectrometer (Pfeiffer-Hakuto OmniStar-s).

2. 3. Characterization

X-ray diffraction (XRD) patterns were recorded with a Rigaku RINT 2500X diffractometer, using monochromatized Cu Kα radiation. Solid-sate ^{51}V MAS NMR (nuclear magnetic resonance) spectroscopy was performed with a Bruker AVANCE DSX 300, using 0.16 M (1 M = 1 mol·dm^{-3}) $NaVO_3$ solution as the external reference at −574 ppm at room temperature and a spinning rate of 25 kHz. X-ray photoelectron spectroscopy (XPS; Shimadzu ESCA-1000AX) was carried out using monochromatized Mg Kα radiation. The binding energies were corrected using 285 eV for C 1s as an internal standard. Specific surface areas were measured by N_2 adsorption at 77 K according to the BET theory (Nippon Bel, BELSORP 18).

3. Results and Discussion

3. 1. Catalytic Activities on VO_x/CaHAp and VO_x/SrHAp

Five types of both VO_x/CaHAp and VO_x/SrHAp catalysts were prepared. The XRD (X-ray diffraction) patterns of four VO_x/CaHAp catalysts were essentially identical to that of CaHAp prepared for this study and agreed with the reference patterns for $Ca_{10}(PO_4)_6(OH)_2$ (JCPDS 09-0432) (**Fig. 1**). Similarly, the XRD patterns of four VO_x/SrHAp catalysts and SrHAp prepared for this study matched the reference data for $Sr_{10}(PO_4)_6(OH)_2$ (JCPDS 33-1348) (**Fig. 2**). **Table 1** shows the *a*-axis and *c*-axis lattice constants of VO_x/CaHAp and VO_x/SrHAp calculated from these XRD data were insensitive to the loading. However, the specific surface area of both VO_x/CaHAp and VO_x/SrHAp catalysts decreased with increased in loading.

Figure 3 illustrates the conversion of propane and selectivity to propylene, CO and CO_2 in the presence of gaseous oxygen in the feedstream at various VO_x/CaHAp loadings. **Table 1** shows the reaction rates per unit of catalyst weight and surface area. The stabilized activity after 6 h on-stream is shown (**Table 2**). Conversion increased with higher loading and reached the maximum at 2.5% VO_x/CaHAp (**Fig. 3**). The reaction rates per unit surface area also increased with loading and reached the maximum at 5.0% VO_x/CaHAp (**Table 1**). Conversion of propane was 5.7%, selectivity to propylene was 21.3%, and the yield of propylene was 1.2% over CaHAp. In contrast, conversion of C_3H_8 was 10.8%, the selectivity to C_3H_6 was 48.1%, and yield of C_3H_6 was 5.2% over 2.5% VO_x/CaHAp. Therefore, VO_x/CaHAp showed improvement in the catalytic properties. However, the catalytic properties did not exceed those of $Mg_2V_2O_7$ (C_3H_8 conversion = 14%, C_3H_6 selectivity = 50.9% and C_3H_6

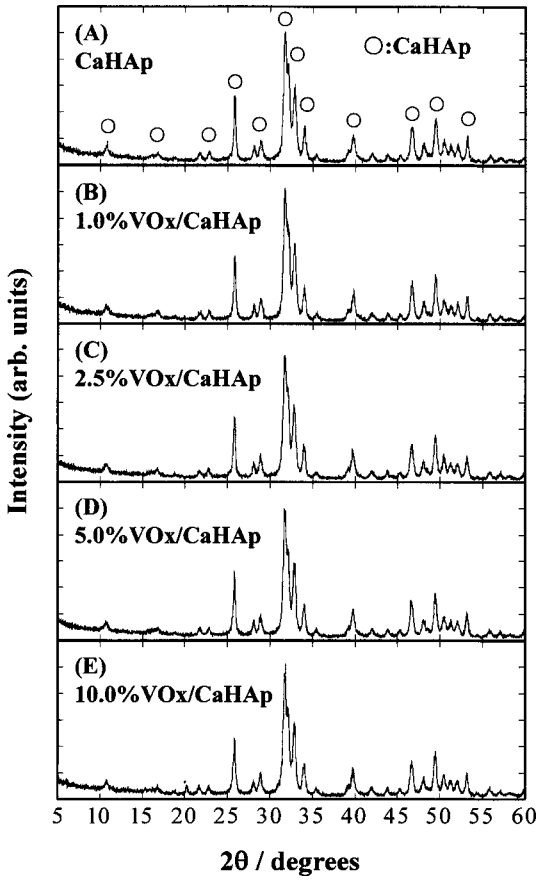

Fig. 1 XRD Patterns of CaHAp and Various VO_x/CaHAp Catalysts before the Use for the Oxidative Dehydrogenation of Propane

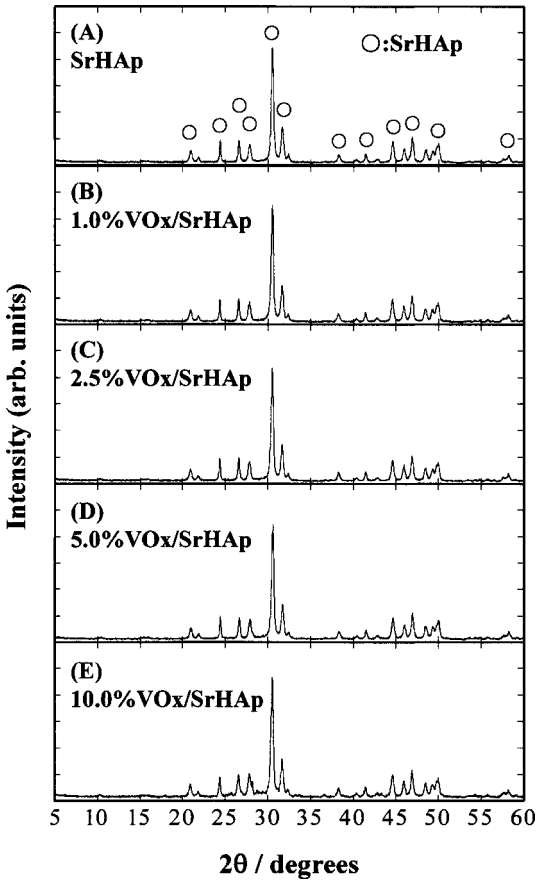

Fig. 2 XRD Patterns of SrHAp and Various VO_x/SrHAp Catalysts before the Use for the Oxidative Dehydrogenation of Propane

Table 1 Lattice Constant, Surface Area and Reaction Rate per Unit of Catalyst Weight and Surface Area for VO_x/CaHAp and VO_x/SrHAp

Catalyst	Lattice constant [nm]		Surface area [m^2/g]	Rate	
	a	*c*		[mol·min^{-1}·g^{-1}]	[mol·min^{-1}·m^{-2}]
CaHAp	0.942	0.687	57	2.01×10^{-5}	3.52×10^{-7}
1.0% VO_x/CaHAp	0.941	0.689	53	3.08×10^{-5}	5.82×10^{-7}
2.5% VO_x/CaHAp	0.943	0.688	53	3.83×10^{-5}	7.23×10^{-7}
5.0% VO_x/CaHAp	0.942	0.690	47	3.76×10^{-5}	8.00×10^{-7}
10.0% VO_x/CaHAp	0.942	0.688	49	3.80×10^{-5}	7.75×10^{-7}
SrHAp	0.976	0.729	35	2.73×10^{-5}	7.79×10^{-7}
1.0% VO_x/SrHAp	0.977	0.729	36	3.27×10^{-5}	9.09×10^{-7}
2.5% VO_x/SrHAp	0.977	0.729	34	4.44×10^{-5}	13.06×10^{-7}
5.0% VO_x/SrHAp	0.978	0.729	34	4.55×10^{-5}	13.38×10^{-7}
10.0% VO_x/SrHAp	0.978	0.730	27	4.08×10^{-5}	16.98×10^{-7}

yield = 7.1%), which is one of the most active catalysts for the oxidative dehydrogenation of propane[10], and CaHAp partly substituted with vanadate (VO_4–CaHAp) (C_3H_8 conversion = 16.5%, C_3H_6 selectivity = 54.2% and C_3H_6 yield = 8.9%) under the same reaction conditions as employed in the present study[2].

Figure 4 illustrates C_3H_8 conversion and selectivity to each product in the presence of gaseous oxygen in the feedstream at various VO_x/SrHAp loadings. The conversion of propane was 7.6%, the selectivity to propylene was 26.7%, and the yield of propylene was 2.0% over SrHAp, all of which were greater than those for CaHAp. Similar effects of loading on the conversion and selectivity to those of VO_x/CaHAp were observed for VO_x/SrHAp, as the selectivity to C_3H_6 was increased and that to CO_2 was decreased extensively by addition of 1.0% vanadate loading. The maximum activity (C_3H_8 conversion = 12.7%, C_3H_6 selectivity =

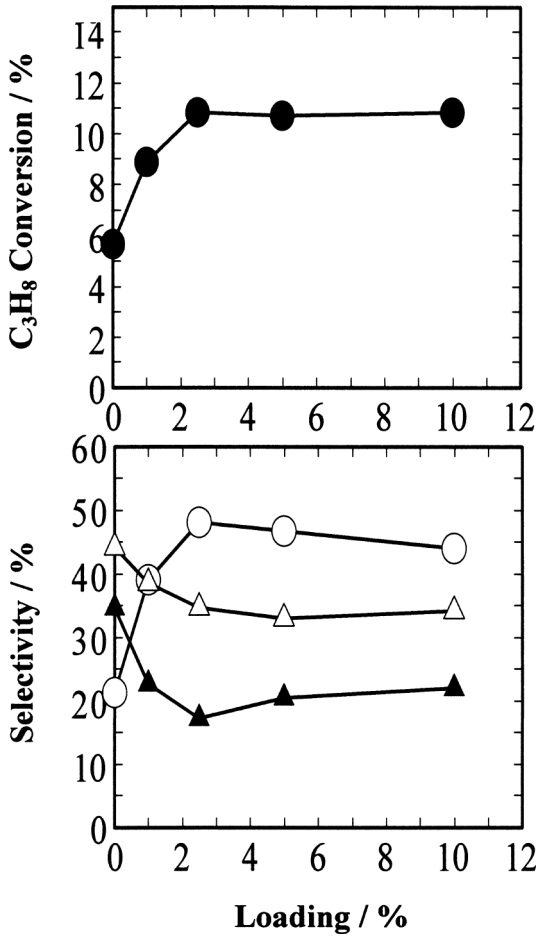

Symbols: (○) C_3H_6 selectivity; (▲) CO selectivity; and (△) CO_2 selectivity.

Fig. 3 Conversion and Selectivity after 6 h on-Stream at 723 K in the Presence of O_2 (4.1 kPa) over CaHAp and VO_x/CaHAp

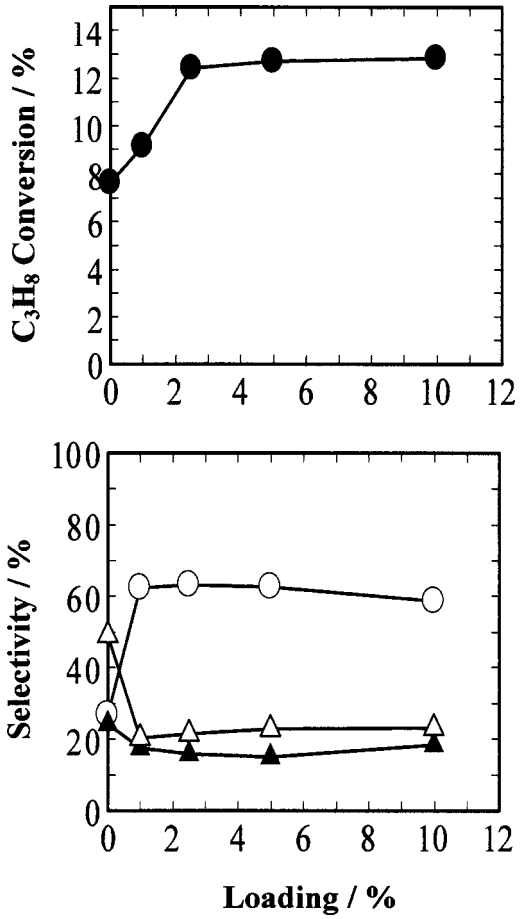

Symbols: (○) C_3H_6 selectivity; (▲) CO selectivity; and (△) CO_2 selectivity.

Fig. 4 Conversion and Selectivity after 6 h on-Stream at 723 K in the Presence of O_2 (4.1 kPa) over SrHAp and VO_x/SrHAp

Table 2 Catalytic Activities over VO_x/CaHAp and VO_x/SrHAp at 0.75 and 6 h on-Stream

Catalyst	Conv. [%]	Selectivity [%]		
	C_3H_8	CO	CO_2	C_3H_6
CaHAp	5.3 (5.7)	37.8 (34.6)	47.0 (44.2)	15.2 (21.3)
1.0% VO_x/CaHAp	8.3 (8.9)	23.2 (22.5)	40.4 (38.5)	36.4 (39.0)
2.5% VO_x/CaHAp	10.4 (10.8)	17.8 (17.4)	36.6 (34.7)	45.5 (48.0)
5.0% VO_x/CaHAp	9.0 (10.7)	21.9 (20.4)	40.7 (33.0)	37.4 (46.6)
10.0% VO_x/CaHAp	8.7 (10.8)	24.6 (21.8)	41.7 (34.2)	33.6 (44.0)
SrHAp	7.1 (7.6)	24.6 (24.2)	49.0 (49.0)	26.4 (26.7)
1.0% VO_x/SrHAp	9.8 (9.1)	18.1 (17.4)	22.8 (20.3)	59.1 (62.3)
2.5% VO_x/SrHAp	11.7 (12.5)	15.1 (15.7)	22.6 (21.3)	62.4 (63.0)
5.0% VO_x/SrHAp	12.5 (13.0)	16.5 (16.7)	24.1 (22.6)	59.4 (60.7)
10.0% VO_x/SrHAp	12.0 (12.8)	18.0 (18.3)	24.5 (23.0)	57.5 (58.7)

Values in parentheses: values at 6 h on-stream.

62.5% and C_3H_6 yield = 7.9%) was observed at 5.0% for VO_x/SrHAp, and was comparable to the activities of $Mg_2V_2O_7$ and VO_4–CaHAp under the same reaction conditions as employed in the present study. As shown in **Figs. 3** and **4**, the conversion and selectivity over VO_x/CaHAp and VO_x/SrHAp were rather insensitive to loading at more than 2.5%, probably due to the reaction conditions close to oxygen-limited conditions since the conversion of oxygen was more than 90% on those catalysts.

The selectivity to C_3H_6 of VO_x/SrHAp was evidently greater than those of $Mg_2V_2O_7$ and VO_4–CaHAp, whereas the order of the reaction rates per unit surface area was $Mg_2V_2O_7 > VO_x$/SrHAp $> VO_4$–CaHAp[2]. Based on our previous studies, oxidative dehydrogenation of methane and propane proceeds favorably over CaHAp and SrHAp, respectively[11),12)], indicating that the active site, the OH group in CaHAp and SrHAp[12)], activates methane and propane at higher and lower reaction temperatures, respectively. Therefore, the beneficial effect of the loading was observed for VO_x/SrHAp rather than for VO_x/CaHAp. This study further investigated the properties of VO_x/SrHAp. The XRD patterns of VO_x/CaHAp and VO_x/SrHAp after use in the oxidative dehydrogenation in the presence of gaseous O_2 were essentially identical to those before the employment of the reaction (not shown).

3. 2. Redox Properties of VO_x/SrHAp

Table 1 shows that the reaction rate per unit surface area increased with higher loading of vanadate. Therefore, the properties of VO_x, rather than the surface area, were the important contributors to the catalytic activity, although the combination of VO_x and SrHAp was essential for the increased activity. We hypothesized that the lattice oxygen in VO_x was the contributory factor in the enhancement of the activity. Therefore, propane conversion in the absence of gaseous oxygen in the feedstream was investigated.

Figure 5 illustrates the conversion of propane as a function of time-on-stream. Conversion was negligible over the catalysts other than 10.0% VO_x/SrHAp, regardless of time-on-stream. Based on the results for VO_x–CaHAp[2)], SrHAp should demonstrate low activity during the initial time-on-stream until 0.45 h because of no abstraction of lattice oxygen from SrHAp, whereas 1.0-5.0% VO_x/SrHAp could be expected to show more activity than SrHAp during the initial time-on-stream until 0.45 h, due to the rapid abstraction of lattice oxygen from VO_x. Therefore, abstraction of lattice oxygen in VO_x is important in the reaction behaviors. If lattice oxygen is abstracted from the catalysts, the structure of VO_x and the valence of vanadium should be strongly influenced by the abstraction of lattice oxygen. The present study analyzed catalysts previously employed under various conditions by XRD, XPS (X-ray photoelectron spectroscopy) and solid-state ^{51}V MAS NMR (nuclear magnetic resonance).

Regardless of the presence or absence of gaseous oxygen in the feedstream, essentially identical XRD patterns to those illustrated in **Fig. 2** were observed for the catalysts after use to obtain the results illustrated in **Figs. 4** and **5** (not shown). XPS was used to investigate the effects of oxygen abstraction from VO_x and the composition over the catalyst surface. **Table 3** lists data for the binding energy of each component and the P/Sr, O/Sr and V/Sr atomic ratios obtained from 10.0% VO_x/SrHAp before and after reactions with and without gaseous oxygen ((A), (B) and (C) in **Table 3**, respectively). Information on VO_x is more easily obtained from a VO_x-rich catalyst, so 10.0% VO_x/SrHAp was analyzed. The binding energy of V $2p_{3/2}$ together with other components and the O/Sr atomic ratio were essentially insensitive to the reaction conditions used.

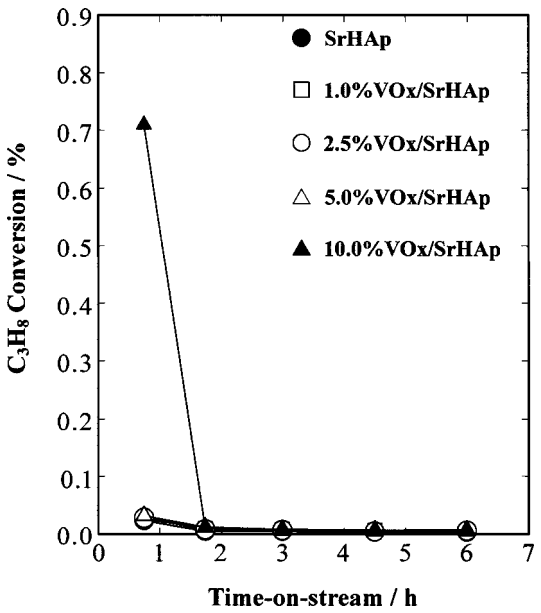

Fig. 5 Conversion of Propane at 723 K in the Absence of O_2 over SrHAp and VO_x/SrHAp

Table 3 Surface Characteristics of 10.0% VO_x/SrHAp before and after Propane Conversion under Various Reaction Conditions

Conditions	Binding energy [eV]				Atomic ratio		
	Sr $3p_{1/2}$	P 2s	O 1s	V $2p_{3/2}$	P/Sr	O/Sr	V/Sr
(A) Before C_3H_8 conversion	280.0	190.8	531.6	517.9	0.30	1.29	0.02
(B) After C_3H_8 conversion at $P(O_2) = 4.1$ kPa	279.5	190.8	531.3	517.4	0.30	1.29	0.02
(C) After C_3H_8 conversion at $P(O_2) = 0$ kPa	279.5	190.3	531.0	517.2	0.32	1.36	0.03
(D) After re-oxidation of the sample used in (C)	279.2	190.5	531.2	517.6	0.33	1.29	0.02

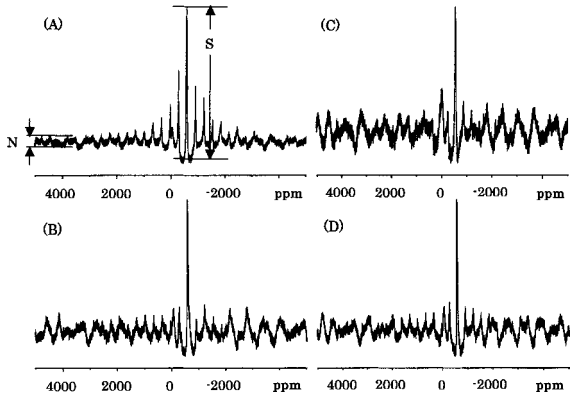

Fig. 6 ^{51}V MAS NMR of 10.0% VO_x/SrHAp before and after Propane Conversion under Various Reaction Conditions: (A) fresh; (B) after propane conversion with oxygen ($P(O_2)$ = 4.1 kPa); (C) after propane conversion without oxygen ($P(O_2)$ = 0 kPa); and (D) after re-oxidation at 723 K for 1 h with O_2 (25 m*l*/min) of the sample used in (C)

Binding energy of V $2p_{3/2}$ from V^{5+} is 517.85, 517.5 and 518.6 eV for V_2O_5 and Na_3VO_4[2),4),13),14)]. Furthermore, a chemical shift of approximately 1 eV occurs between V^{5+} (V_2O_5) and V^{4+} (VO_4) in XPS analysis (516.8 and 515.7 eV)[4),15),16)]. Therefore the valence of vanadium over the catalyst was +5, even after propane conversion in the absence of gaseous oxygen in the feedstream, due to the supply of oxygen species from the bulk to the surface. Abstraction of lattice oxygen from the surface of 10.0% VO_x/SrHAp should reduce the atomic ratio of O/Sr after use for propane conversion without gaseous oxygen. However, the O/Sr ratio after propane conversion without gaseous oxygen was essentially identical to the other conditions, again indicating that oxygen species were supplied from the bulk to the surface.

The XRD and XPS analyses provided no direct evidence for the abstraction of lattice oxygen from the catalyst, so solid-state ^{51}V MAS NMR was performed. If the lattice oxygen in VO_x is abstracted, the valence of vanadium should be reduced from 5+ to 4+. Solid-state ^{51}V MAS NMR is suitable for observing the reduction of vanadium, since NMR can detect vanadium 5+ but not vanadium 4+. We previously found that the redox behaviors of vanadium species can be reasonably explained by the combination of XRD, EXAFS (extended X-ray absorption fine structure) and solid state ^{51}V MAS NMR[17)]. Therefore ^{51}V MAS NMR was used to examine the redox behaviors of vanadium species. **Figure 6** illustrates ^{51}V MAS NMR obtained for 10.0% VO_x/SrHAp: as unused; after propane conversion with oxygen; and, after propane conversion without oxygen. The fresh catalyst demonstrated an evident NMR signal due to vanadium at −596 ppm together with various side bands (**Fig. 6 (A)**). The ^{51}V MAS NMR signal due to V_2O_5, which has been extensively studied as a model catalyst for the oxidative dehydrogenation of propane[18),19)], occurs at −609 ppm, indicating that VO_x on the supported catalyst is not a simple oxide. In this study, the signal/noise ratio (S/N) was used to estimate the conversion of V^{5+} to V^{4+}. As illustrated in **Figs. 6 (A)** and **(B)**, the S/N ratio of the fresh catalyst was approximately 12, but became 3.6 after propane conversion with O_2, indicating that slight reduction of V^{5+} to V^{4+} proceeds even in the presence of gaseous oxygen. Further reduction to V^{4+} was detected after propane conversion without O_2 in the feedstream (**Fig. 6 (C)**), shown by the S/N ratio of approximately 3.0. Therefore, abstraction of lattice oxygen, followed by reduction of V^{5+} to V^{4+}, was confirmed in VO_x/SrHAp catalysts. If the VO_x species has a favorable redox chracteristics, the V^{4+} species in sample **(C)** in **Fig. 6** should be converted to V^{5+} species by re-oxidation. Indeed, the S/N ratio became approximately 5.1 after the re-oxidation, at 723 K for 1 h with O_2 (25 m*l*/min), of sample **(C)** in **Fig. 6**, indicating that part of the V^{4+} was converted into the V^{5+} species. As described in (D) in **Table 3**, the valence of the vanadium species over the catalyst surface was 5+ during the reduction/re-oxidation cycles in this study, due to the supply of oxygen from the bulk to the surface.

Reduction of a V^{5+} to a V^{4+} species in VO_x/SrHAp results in the formation of oxygen vacancy due to the abstraction of lattice oxygen in the catalysts. Re-oxidation of the reduced catalysts should be dissimilar, so detection of the effects of loading of the catalysts during re-oxidation may be possible. Therefore, the catalysts were employed for the propane conversion in the absence of oxygen in the feedstream ($P(C_3H_8)$ = 14.4 kPa diluted with He, F = 30 m*l*/min, T = 723 K and W = 0.25 g) for 1.5 h on-stream, followed by the introduction of oxygen ($P(O_2)$ = 4.1 kPa) into the feedstream (**Fig. 7**). The quadrupole mass spectrometer was used to analyze the oxygen-response in the effluent gas. **Figure 7** shows the oxygen-responses after the introduction of oxygen to SrHAp and to various VO_x/SrHAp; t = 0 min in **Fig. 7** corresponds to the above-described 1.5 h on-stream. Although evident information, as observed from a similar experiment using magnesium vanadate[20)], was not observed, oxygen was detected first at *ca.* 30 s on SrHAp, which showed the lowest activity for oxidative dehydrogenation, whereas oxygen was last detected at *ca.* 40 s for 5.0% VO_x/SrHAp, which showed the maximum activity in this study. Clearly the detection time of oxygen effluent for various VO_x/SrHAp catalysts was later than that for SrHAp, indicating that the lattice oxygen in VO_x directly contributes to the activation of C_3H_8.

3. 3. Reaction Mechanism

To evaluate the basic properties of VO_x/SrHAp and investigate the reaction mechanism for the oxidative dehydrogenation of propane, the effects of $P(C_3H_8)/P(O_2)$

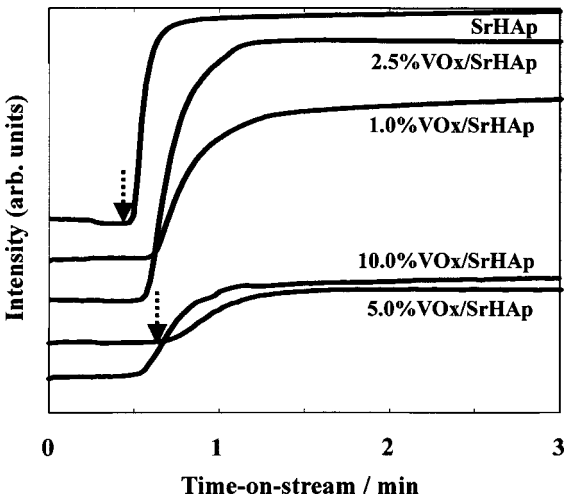

Reaction conditions: before and after $t = 0$ min, the catalysts (0.25 g) were exposed to the reactant gas ($P(C_3H_8) = 14.4$ kPa diluted with He; $T = 723$ K; $F = 30$ m*l*/min) in the absence ($P(O_2) = 0$ kPa) and presence of O_2 ($P(O_2) = 4.1$ kPa), respectively.

Fig. 7 Oxygen Response in the Effluent Gas from SrHAp and Various VO_x/SrHAp Catalysts

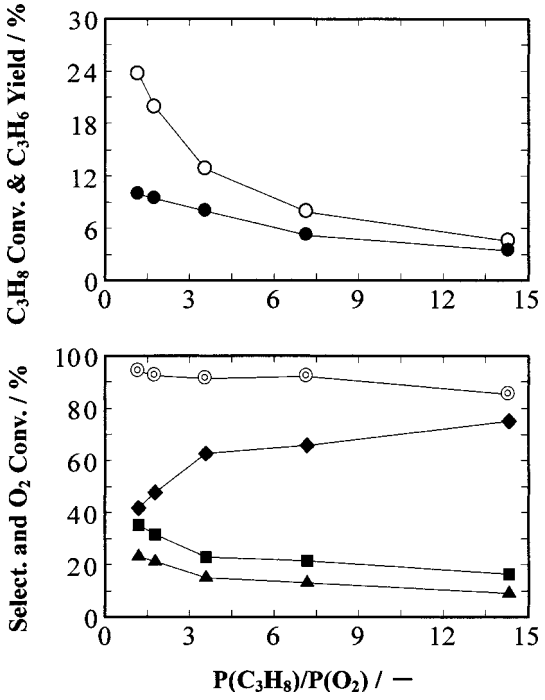

Symbols: (○) C_3H_8 conversion; (●) C_3H_6 yield; (◆) C_3H_6 selectivity; (■) CO_2 selectivity; (▲) CO selectivity; (◎) O_2 conversion.

Fig. 8 Effect of $P(C_3H_8)/P(O_2)$ on the Oxidative Dehydrogenation of Propane over 5.0% VO_x/SrHAp at 723 K at 6 h on-Stream

and W/F were observed for 5.0% VO_x/SrHAp. $P(C_3H_8)/P(O_2)$ ratios of 28.8/2.1, 28.8/4.1, 14.4/4.1, 14.4/8.2 and 14.4 kPa/12.3 kPa were used, diluted with He. As expected, increased $P(C_3H_8)/P(O_2)$ ratio resulted

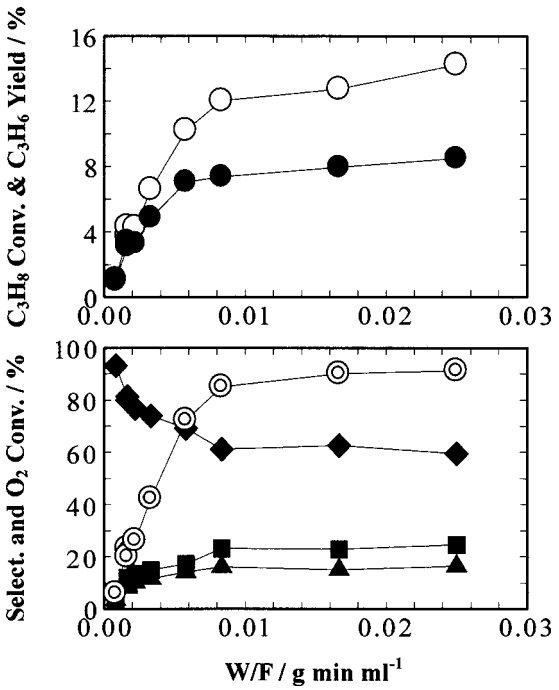

Symbols: (○) C_3H_8 conversion; (●) C_3H_6 yield; (◆) C_3H_6 selectivity; (■) CO_2 selectivity; (▲) CO selectivity; (◎) O_2 conversion.

Fig. 9 Effect of W/F on the Oxidative Dehydrogenation of Propane over 5.0% VO_x/SrHAp at 723 K at 6 h on-Stream

in increased selectivity to C_3H_6 and decreased conversion of C_3H_8 as illustrated in **Fig. 8**. However, the yield of C_3H_6 increased with lower $P(C_3H_8)/P(O_2)$ ratios, indicating that gaseous oxygen in the feedstream promoted the oxidative dehydrogenation of C_3H_8 to C_3H_6 rather than deep oxidation to CO_x. **Figure 9** shows that the catalytic activities for $W/F = 0.0083$, 0.0167 and 0.0250 were almost identical. However, conversions of C_3H_8 and O_2 decreased at $W/F = 0.0056$ or lower. Almost total O_2 conversion was achieved at $W/F = 0.0083$ and higher, with no further change in conversion with increased amount of catalyst, indicating that excess 5.0% VO_x/SrHAp does not promote the oxidation of propane. **Figure 7** shows that the selectivities to C_3H_6 and CO_x increased to 100% and decreased to 0%, respectively, with decreasing W/F ratio, indicating that propylene was first formed on the catalyst, followed by deep oxidation to CO_x in the oxidative dehydrogenation of propane over 5.0% VO_x/SrHAp.

4. Conclusions

The present study showed that vanadate catalyst supported on strontium hydroxyapatite was active for the oxidative dehydrogenation of propane. The redox properties of the vanadate species, combined with the properties of the OH groups of strontium hydroxyapatite, compared to those of calcium hydroxyapatite,

directly contributed to the increased activity of the supported catalyst. Easy abstraction and incorporation of lattice oxygen from and into vanadate, respectively, on VO_x/SrHAp, as indirectly expected from the redox behaviors of the vanadium species demonstrated by ^{51}V MAS NMR, resulted in favorable redox cycles for the oxidative dehydrogenation of propane to propylene.

References

1) Sugiyama, S., Osaka, T., Hashimoto, T., Sotowa, K.-I., *Catal. Lett.*, **103**, 121 (2005).
2) Sugiyama, S., Osaka, T., Hirata, Y., Sotowa, K.-I., *Appl. Catal. A: General*, **312**, 52 (2006).
3) Chaar, M. A., Patel, D., Kung, H. H., *J. Catal.*, **109**, 463 (1988).
4) Sam, D. S. H., Soenen, V., Volta, J. C., *J. Catal.*, **123**, 417 (1990).
5) Bettahar, M. M., Costentin, G., Savary, L., Lavalley, J. C., *Appl. Catal. A: General*, **145**, 1 (1996).
6) Pak, C., Bell, A. T., Tilley, T. D., *J. Catal.*, **206**, 49 (2002).
7) Hayek, E., Newesely, H., *Inorg. Synth.*, **7**, 63 (1963).
8) Matsumura, Y., Sugiyama, S., Hayashi, H., Shigemoto, N., Saitoh, K., Moffat, J. B., *J. Mol. Catal.*, **92**, 81 (1994).
9) Hattori, T., in: Catalysis Society of Japan (Ed.), "Shokubai Sekkei," Kodansha, Tokyo (1989), p. 163.
10) Kung, H. H., *Adv. Catal.*, **40**, 1 (1994).
11) Sugiyama, S., Minami, T., Moriga, T., Hayashi, H., Koto, K., Tanaka, M., Moffat, J. B., *J. Mater. Chem.*, **6**, 459 (1996).
12) Sugiyama, S., Shono, T., Makino, D., Moriga, T., Hayashi, H., *J. Catal.*, **214**, 8 (2003).
13) Wagner, C. D., Riggs, W. M., Davis, L. E., Moulder, J. F., Muilenberg, G. E., "Handbook of X-ray Photoelectron Spectroscopy," Physical Electronics Division, Perkin-Elmer Corporation, Eden prairie, MN (1979).
14) Nefedov, V. I., Firsov, N. M., Shaplygin, I. S., Electr, J., *Spectrosc. Relat. Phenom.*, **26**, 65 (1982).
15) McIntyre, N. S., Chan, T. C., in: Briggs, D., Seah, M. P., (Eds.), second ed., "Practical Surface Analysis," Vol. 1, John Wiely & Sons, Chichester (1990), p. 502.
16) Blaauw, C., Leenhouts, F., van der Woode, F., Sawatzky, G. A., *J. Phys. C*, **8**, 459 (1976).
17) Sugiyama, S., Osaka, T., Hirata, Y., Kondo, Y., Nakagawa, K., Sotowa, K.-I., *J. Chem. Eng. Jpn.*, in press.
18) Barbero, B. P., Cadus, L. E., Hilaire, L. U., *Appl. Catal. A: General*, **246**, 237 (2003).
19) Kondratenko, E. V., Ovsitser, O., Radnik, J., Schneider, M., Kraehnert, R., Dingerdissen, U., *Appl. Catal. A: General*, **319**, 98 (2007).
20) Sugiyama, S., Hashimoto, T., Tanabe, Y., Shigemoto, N., Hayashi, H., *J. Mol. Catal., A*, **227**, 255 (2005).

……

要　　旨

カルシウムおよびストロンチウムヒドロキシアパタイト担持バナデート触媒によるプロパンの酸化脱水素反応

杉山　　茂[†1),†2),†3)]，逢坂　岳士[†3)]，上野　洋平[†3)]，外輪　健一郎[†1),†2),†3)]

[†1)] 徳島大学大学院ソシオテクノサイエンス研究部 先進物質材料部門，770-8506 徳島市南常三島町2-1

[†2)] 徳島大学大学院ソシオテクノサイエンス研究部 フロンティア研究センター 地圏環境エネルギー部門，770-8506 徳島市南常三島町2-1

[†3)] 徳島大学工学部化学応用工学科，770-8506 徳島市南常三島町2-1

プロパンからプロピレンへの酸化脱水素反応がカルシウムおよびストロンチウムヒドロキシアパタイト担持バナデート触媒（VO_x/CaHAp，VO_x/SrHAp）を用いて検討された。バナデートを担持することによって活性が改善されたが，特に VO_x/SrHAp で顕著な活性改善が見られた。5% VO_x/SrHAp 触媒を用いた場合のプロピレン収率は，従来最高活性を与える触媒の一つと言われていた $Mg_2V_2O_7$ に匹敵する収率を示した。ヒドロキシアパタイトの活性座である OH 基とバナデートの複合作用によって高活性が得られることが示された。さらに，バナデートのレドックスの性質が触媒活性に反映することも確認された。接触時間の反応挙動に対する効果から，プロパンが酸化脱水素され，まずプロピレンが形成され，さらにプロピレンの再酸化によって CO_x が生成し，プロパンから直接 CO_x が生成しないことが明らかになった。

……